Precision Engineering 37 (2013) 364–371

Contents lists available at SciVerse ScienceDirect

Precision Engineering

journal homepage: www.elsevier.com/locate/precision

Development of a tertiary motion generator for elliptical vibration texturing

Ping Guo [a,*], Kornel F. Ehmann [b]

[a] Department of Mechanical Engineering, Northwestern University, 2145 Sheridan Road, Room B110, Evanston, IL 60208, USA
[b] Department of Mechanical Engineering, Northwestern University, 2145 Sheridan Road, Room A215, Evanston, IL 60208, USA

ARTICLE INFO

Article history:
Received 15 May 2012
Received in revised form 20 August 2012
Accepted 9 October 2012
Available online 23 October 2012

Keywords:
Elliptical vibration texturing
Elliptical vibration cutting
Tertiary motion generator
Modal analysis
Langevin transducer
Piezo actuator

ABSTRACT

The elliptical vibration texturing process is an innovative machining method for the fast generation of textured surfaces. It adds a tertiary motion component to the tool tip, which introduces deliberate elliptical vibrations between the cutting tool and the workpiece. The elliptical locus lies in the plane that is defined by the cutting direction and the radial direction in the turning operation. This paper proposes a new design for a resonant mode 2D tertiary motion generator (TMG) that can deliver the required elliptical trajectory at an ultrasonic frequency. The device works in the resonant mode, with tangential and normal vibrations at a nearly identical resonant frequency. Simulation and experiments were carried out to perform a modal analysis of the system. Different design parameters were adjusted to achieve large vibration amplitudes in both tangential and normal directions. The elliptical vibration texturing process was implemented by integrating the newly developed TMG into a turning operation. Preliminary test results of dimple array patterns are presented that validate the performance and principle of the proposed design.

1. Introduction

Surface textures have a decisive impact on the functional performance of products. Proper patterns on structured surfaces could dramatically improve their optical, mechanical, thermal, and biological properties [1]. These structured surfaces usually have periodic patterns with micro/meso-scale features that cannot be fully described by conventional surface topography parameters, such as roughness and waviness. Applications of structured surfaces include friction reduction, heat exchange, optical gratings, superhydrophobic surfaces, etc.

How to accurately and efficiently generate micro-structures on engineered surfaces are a big challenge as well as a timely research topic. At the micro-scale, laser ablation is favorable for its flexibility, but it is usually limited to the prototyping stage because of its high cost and long processing time. It is also limited to non-transparent materials and needs further post-processing. The micro forming method is ideal for mass production; however, it has difficulties with high strength and brittle materials. Besides, how to manufacture the molds with micro features remains a problem.

Micro-machining is well suited at this length scale. It offers significant advantages for its flexibility to process all work materials [2]. Micro-machining with diamond tools, for example, can provide nanometric surface finish without requiring post-processing operations as compared to laser ablation. It increases the geometric accuracy since it eliminates remounting and further operations that degrade accuracy. Currently, however, the only way to machine 3D micro-features is by 5-axis NC controlled machining. Although this method is very accurate, the processing time is not acceptable for mass production.

From the analysis above, it is evident that currently there is limited ability to accurately machine micro-structure features on 3D free-form surfaces, especially at a mass production scale. The limitations in various existing processes for micro-texturing call for a novel machining process, which motivates this paper.

The objective of this paper is to implement an innovative machining method for the fast generation of textured surfaces: *the elliptical vibration texturing process*. The core part of the problem is the development of the tertiary motion generator (TMG) that can generate elliptical vibration trajectories at ultrasonic frequencies. The paper is organized as follows: first, the elliptical vibration texturing process is introduced. Then the development of the TMG is described in detail along with a simulation and experimental analysis. Finally, preliminary experimental results using this newly developed process are presented and followed by conclusions.

2. Elliptical vibration texturing process

The elliptical vibration texturing process originates from the surface-shaping system proposed by Hong and Ehmann [3]. It adds to the cutting tool tip a tertiary motion component, which is a

* Corresponding author. Tel.: +1 847 467 1851; fax: +1 847 491 3915.
E-mail addresses: Pingguo2009@u.northwestern.edu, steven.guoping@gmail.com (P. Guo), k-ehmann@northwestern.edu (K.F. Ehmann).

0141-6359/$ – see front matter © 2012 Elsevier Inc. All rights reserved.
http://dx.doi.org/10.1016/j.precisioneng.2012.10.005

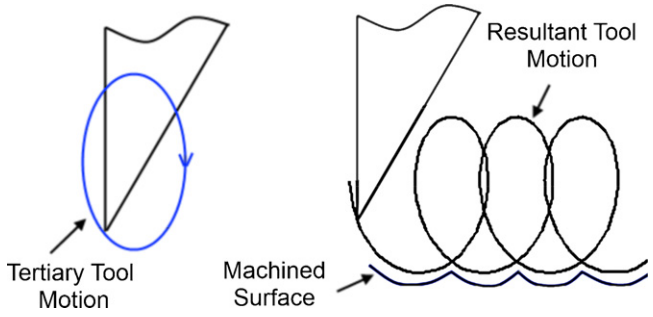

Fig. 1. Principle of the elliptical vibration texturing process.

higher order motion superimposed on the conventional primary and secondary, i.e., cutting and feed motions. It introduces deliberate and controllable vibrations between the cutting tool and the workpiece. The principle of process is shown in Fig. 1. The cutting tool vibrates along a prescribed trajectory with amplitudes of several microns (e.g., an elliptical trajectory as shown in the figure). The resultant tool path imposes textures, i.e., dimples, onto the workpiece surface. The shape and pattern of the texture depend on the shape of the vibration trajectory (the tertiary motion), the cutting speed and feed rate (primary and secondary motions), as well as on tool geometry.

This process is inspired by the idea of the elliptical vibration assisted cutting (EVC) process. Early EVC processes utilized one-dimensional vibrations in the cutting direction, turning the continuous cutting process into an intermittent process. The vibration frequency is usually in the ultrasonic regime, ranging from 20 kHz to 50 kHz. Moriwaki and Shamoto [4] first applied one-dimensional ultrasonic vibration cutting to turning operations. They were able to machine ferrous materials by diamond tools and to achieve optical quality surfaces. Later, they have proposed the idea of EVC, which introduces tool vibrations in both the cutting and chip flow directions in the orthogonal cutting model [5]. This arrangement significantly reduces the instantaneous chip thickness and brings various benefits such as reduced cutting forces, better surface finish, burr suppression, and longer tool life [4–10]. The EVC process also offers advantages in the ductile-regime cutting of brittle materials. It remarkably increases the critical depth of cut, below which the brittle material deforms plastically and forms a crack-free surface [11,12]. Kim and Loh [13] have applied the EVC process to machining micro-channels and pyramidal patterns. Their results have shown significant improvements in surface quality and form accuracy.

The cylindrical turning operation shown in Fig. 2 depicts the difference between the EVC and the elliptical vibration texturing process. Unlike the EVC process, the elliptical vibration texturing process adds vibrations in the cutting and radial directions, while in the EVC process the vibrations are in the cutting and feed directions. The radial vibration dictates the texturing process by varying the cutting depth in the turning operation. The vibration in the cutting direction gives the possibility for generating more complicated texture shapes and patterns. It also brings the benefits of vibration assisted machining into the texturing process, which could lead to the texturing of brittle materials.

3. Development of a resonant mode 2D TMG

The design of the TMG is the key technological problem in the implementation of the elliptical vibration texturing process. There are two possible working principles for the design: the resonant mode and the non-resonant mode. Each working principle has its own advantages and limitations. The resonant TMG works at discrete natural frequencies of the system structure; the

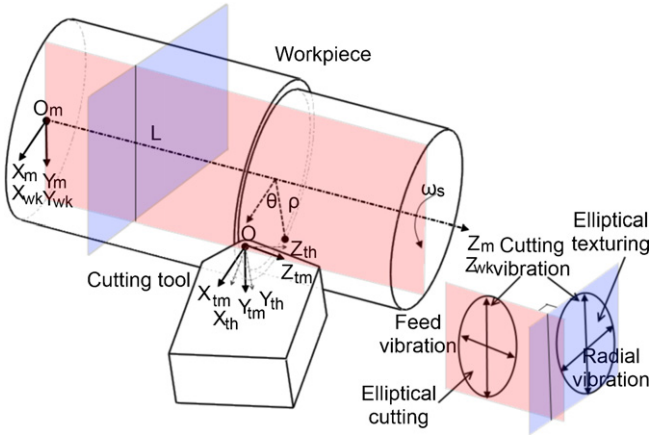

Fig. 2. Illustration of the elliptical vibration texturing process in cylindrical turning operations.

non-resonant TMG works in a continuous frequency range. The resonant TMG is able to achieve a higher operating frequency and is more energy efficient, but a precise control of the trajectory is more difficult owing to the nature of the resonant vibrations and the phase lag between the excitation and mechanical response. The non-resonant TMG is not limited to a fixed operating frequency and offers a more precise control of the motion. It also has the potential to create an arbitrary motion trajectory for complex texture patterns. It is, however, very difficult to achieve a high operating frequency because of various technical problems involved. The scope of this paper focuses on the development of the resonant mode TMG.

3.1. Literature review

The current state-of-the-art design of a resonant mode TMG, which generates an elliptical trajectory, lies in the fields of EVC and ultrasonic motors. A resonant transducer that produces elliptical vibrations at ultrasonic frequencies was developed by Moriwaki and Shamoto [6]. The system is shown in Fig. 3(a). Piezoelectric plates are attached to four sides of a beam. The bending modes in both horizontal and vertical directions are excited by applying alternate sinusoidal voltages to the four piezoelectric plates. Two bending vibrations with proper phase difference cause the diamond

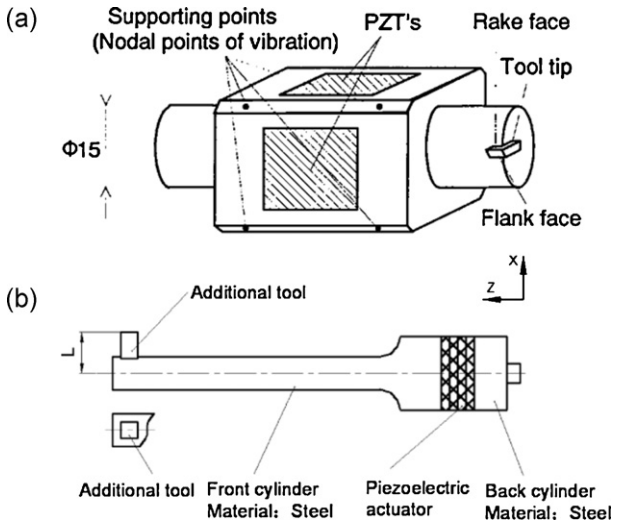

Fig. 3. Traditional resonant transducer designs: (a) Moriwaki and Shamoto's design [6] and (b) Li's design [7].

cutting tip to vibrate along an elliptical locus. The vibration amplitudes are 4 μm in both directions; and the natural frequency is 20 kHz. Li and Zhang [7] developed an ultrasonic elliptical vibration transducer using a single piezoelectric actuator. The radially asymmetric structure results in a longitudinal-bended compound vibration mode (shown in Fig. 3(b)). The transducer generates vibration amplitudes of 16 μm in the cutting direction and 2 μm in the feed direction at its natural frequency of 22.5 kHz. Kim and Loh [13] developed an elliptical vibration generator for micro-grooving applications. The device is excited at 18 kHz, producing vibration amplitudes of 2 μm × 1 μm. There is also a commercial EVC device, EL-50, available from Taga Electric Co., Ltd., which generates vibration amplitudes of 4 μm at 39 kHz [14].

The design proposed in the current work was inspired by the design of Kuribayashi Kurosawa et al. [15] of an ultrasonic motor. Similar designs, also based on Kurosawa's concept, were developed by Zhang et al. [16] and Asumi et al. [17] who further miniaturized this design. Design based on this concept could produce large vibration amplitudes in a compact size; however, these devices were specifically designed for ultrasonic motor applications by focusing on the maximal output speed, force, and mechanical power. In surface texturing applications the shape and vibration amplitudes of the elliptical locus are more important.

3.2. Design and principle of operation

The current design is composed of two bolt-clamped Langevin transducers. Each transducer includes two PZT rings. The PZT rings have an outer diameter of 14.5 mm, an inner diameter of 7 mm and a thickness of 5 mm. The PZT materials are of Navy Type I and manufactured by NTK technologies, Inc. The CAD model of the device is shown in Fig. 4. The base block connects two transducers to provide a fixed node. Each transducer is a standard Langevin transducer connected at one end by a head block (flexure structure). The angle between the two transducers is held at 60° in the present design to reduce its overall size. The envelope dimension of the ultrasonic device is about 100 mm × 100 mm × 40 mm. Two end masses at the other end of the transducers provide the preload to the PZT rings. The diameter of the end mass is fixed at 15 mm. The length of the end mass serves as a control parameter to adjust the natural frequencies of the system and is optimized to be 37 mm. The head block serves as a tool holder, as well as a clamp for the PZT rings. The flexure hinge design in the head block helps to amplify the vibrations in the tangential and normal directions and minimizes the motion in the thickness direction.

The TMG works in the resonant mode. The two symmetric Langevin transducers are driven by harmonic signals at the natural frequencies of the system. The longitudinal vibrations of the two transducers are joined and magnified by the flexure structure of the head block leading to tool tip movements along elliptical trajectories.

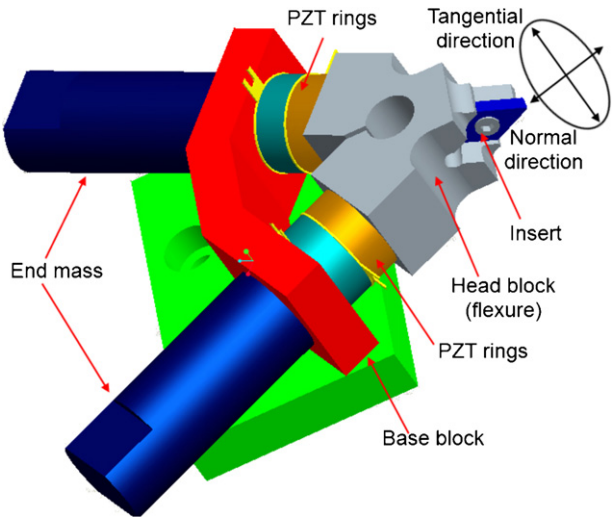

Fig. 4. Design of the TMG.

The complex mechanical structure of the device leads to multiple vibration modes. The two main vibration modes associated with the flexure structure are the tangential (Fig. 5(a)) and the normal direction vibrations (Fig. 5(b)). The tangential vibration mode occurs when the longitudinal vibrations of the two transducers are out of phase. The anti-phase mode causes asymmetric vibration of the flexure accompanied by large shear deformation in the flexure structure. The normal vibration mode occurs when the two longitudinal vibrations are in phase. The in-phase mode causes symmetric vibrations of the flexure that result in motions of the tip along the normal direction. In order to generate an elliptical trajectory, the transducers are carefully designed and adjusted such that the above two vibration modes occur approximately at the same frequency.

Several factors determine the resonant frequencies and the vibration amplitudes of the device. The mass distribution of the system predominantly determines the natural frequencies and the mode shapes. This is thoroughly analyzed by finite element simulation in the following section. Assuming that the main structure of the device remains unchanged, the length of the end mass and the cutting insert used could tweak the performance of the device. The structural damping is another important factor that has a major effect on the vibration amplitudes and a minor effect on the natural frequencies; however, the actual damping ratio is difficult to quantify. The preload applied on the PZT rings is one parameter that changes the damping ratio of the structure. There exists an optimum range of the preload for maximal vibration amplitudes. The last factor is the nature of the excitation signals, namely the excitation amplitudes and the relative phase angle between the two inputs. It impacts the vibration amplitudes and phase angle

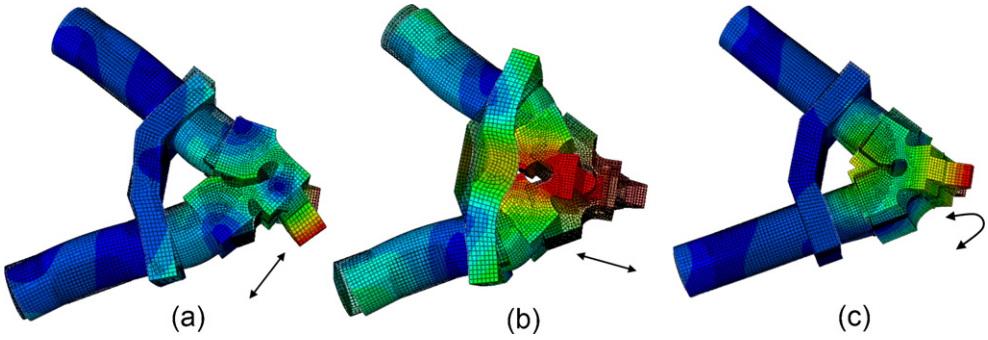

Fig. 5. (a) Tangential vibration mode shape, (b) normal vibration mode shape, and (c) spurious mode shape.

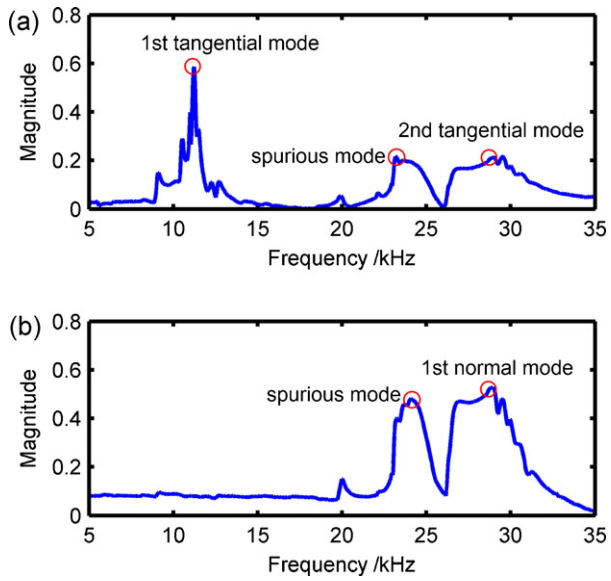

Fig. 6. Sine sweep response: (a) tangential direction and (b) normal direction.

between the two vibration outputs and, thus, changes the shape of the elliptical trajectory. This paper focuses on the analysis of the first and the third factor, namely, the mass distribution and excitation signals, through simulation and experimental assessment.

4. TMG modal analysis

Finite element method (FEM) simulations and experiments were conducted to identify the different vibration modes of the TMG. In the natural frequency extraction simulations, the encastre boundary condition was applied to the bottom side of the base block. Two main resonant frequencies of the system associated with the flexure structure were identified in the analysis and verified through experimental evaluations. There is also a spurious mode associated with the tool tip [17]. In this mode, the flexure structure is not excited, but the tool tip vibrates in a direction perpendicular to the tangential and normal directions as shown in Fig. 5(c). This mode is not desirable in the current application but its effect is negligible.

From the simulation results, the first resonant frequency occurs at 12.96 kHz. The mode shape contains only the tangential vibration mode (Fig. 5(a)), which is referred as the 1st tangential mode. The 1st normal vibration mode, Fig. 5(b), is found at 32.37 kHz while the 2nd tangential vibration mode, Fig. 5(a), at 32.41 kHz. The latter two mode shapes have similar frequencies. The spurious mode, shown in Fig. 5(c), is found at 22.90 kHz from the simulation and is identified at 24.3 kHz in the experiments.

A sine sweep test was performed by applying sinusoidal excitation signals with continuously varying frequency. The frequency range was chosen to be from 5 kHz to 35 kHz. The vibration responses in two directions were recorded and analyzed by FFT. The results are plotted in Fig. 6(a) and (b). The first and third peaks in the tangential direction response correspond to the 1st and 2nd tangential modes. The second peak in the normal direction response corresponds to the 1st normal mode. The second peak in Fig. 6(a) and the first peak in Fig. 6(b) are the spurious mode. These results are in accordance with the FEM analysis. The comparison between the simulation results and experimental observations is listed in Table 1. Here only the tangential and normal modes are of interest. The simulation results match very well with the experiments for the 1st tangential mode. At the 2nd tangential and 1st normal modes, the simulated resonant frequencies are very close (32.37 kHz and 32.41 kHz). In the experiment, these two modes are so coupled that they cannot be differentiated in frequency. This resonant frequency for both the 2nd tangential and 1st normal modes is recorded at 28 kHz, which deviates about (15%) from the simulation results. This is due to: (1) the simplification in the FEM model, including the simplified geometry and the missing damping ratio; (2) the asymmetry in the actual device due to the cutting insert and manufacturing tolerances; (3) the pre-stress effect on the PZT rings, which is not included in the simulation. Despite of the difference in resonant frequencies from the experimental results, the simulations provide useful indication on how closely the 1st normal and 2nd tangential modes are coupled.

Table 1
FEM simulation and modal test comparison.

	Simulation (kHz)	Experiment (kHz)
1st tangential mode	12.96	13.0
1st normal mode	32.37	28.0
2nd tangential mode	32.41	
Spurious mode	22.90	24.3

At the resonant frequency of 28 kHz, the system vibrations possess both the normal and tangential modes. These coupled resonant vibrations generate the desired elliptical locus at the tool tip. In order to obtain large vibration amplitudes in two directions, the normal and tangential mode frequencies should be as close as possible. This is achieved by adjusting the most suitable design parameters, namely, the length of the end mass. The resonant frequencies of the normal and tangential modes change at a different rate, when the length of the end mass changes. So, there exists an optimum length at which the two resonant frequencies cross each other. This condition was studied through FEM simulations described next.

The simplified CAD model of the TMG combines the cutting insert and the tool holder. The equivalent tool is attached to the head block and takes the length of 11.5 mm (this length is defined as the equivalent tool length). The length of the end mass is taken as the control parameter in the natural frequency extraction analysis. The frequencies of the two tangential modes and of the normal mode in question are recorded and plotted in Fig. 7. The general trends of the resonant frequencies show a decrease as the length of the end mass increases. The 1st normal and 2nd tangential modes are very close to each other in their respective resonant frequencies when the end mass length is in the range of 35–40 mm. The current design is based on 37 mm, which is in the optimal range.

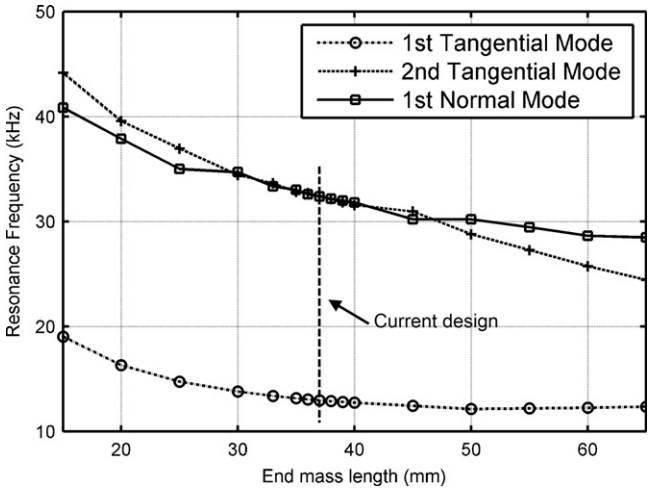

Fig. 7. Influence of end mass length on the resonant frequency.

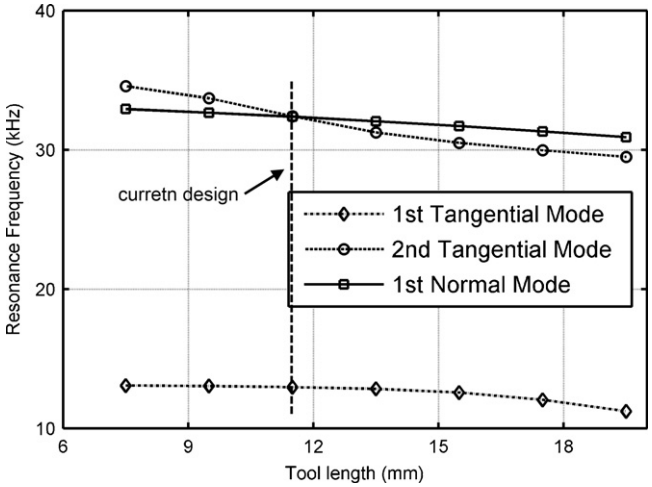

Fig. 8. Influence of tool length on the resonant frequency.

The tool length also affects the vibration behavior of the device. When the end mass length is set at 37 mm, by varying the equivalent tool length in the simulation, the resonant frequencies of the three different modes are plotted in Fig. 8. The general trend is similar to the previous one, i.e., the resonant frequency decreases when the tool length increases. The current value of 11.5 mm of the tool length is around the optimal, as defined by the point where the two lines of the resonant frequencies cross each other.

5. TMG performance assessment

5.1. Experimental setup

The experimental setup is shown in Fig. 9. The excitation signals are generated by a National Instrument data acquisition card (NI DAQ PCIe-6361), which has two analog outputs. The output signal is sampled at 1.5 MHz to ensure the necessary smoothness. The phase difference between the two excitation signals can be set arbitrarily using the Labview program. The excitation signals are sent to a piezo amplifier (TREK PZD 350), which has a 0 to ±350 V bipolar output and a fast response given by a 500 V/μs slew rate. The high-voltage two-channel sinusoidal signals (V_{pp} = 625 V) are supplied to the two Langevin transducers. The motion of the tool tip is monitored by MicoSense capacitance sensors, whose range of measurement is 100 μm. The sensor has a sub-nanometer resolution and 100 kHz bandwidth. An orthogonal block is placed into the insert holder as a target for displacement sensing. The vibration

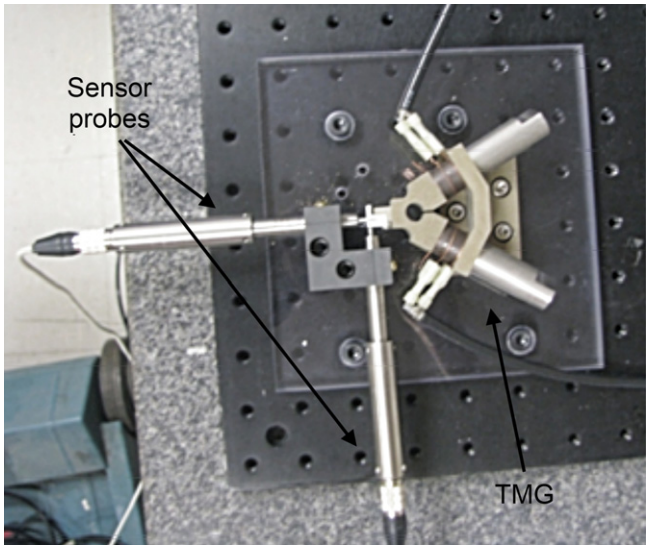

Fig. 9. Experimental setup.

data are recorded using the same data acquisition card (NI PCIe-6361) at a 500 kHz sampling frequency.

5.2. Performance analysis

The performance of the TMG was evaluated through measurements of the tool tip trajectory at its natural frequencies. By the sine sweep test, two major peaks associated with the normal and tangential modes were found as predicted by the simulation. The system's displacement response in two directions at its 1st resonant frequency of 13 kHz is shown in Fig. 10(a). The tangential vibration amplitude is 26.17 μm; and the normal vibration amplitude is 7.95 μm. The 2D trajectory is then plotted and fitted to an ellipse function, as shown in Fig. 10(b). The ellipse has a major axis of 28.74 μm, a minor axis of 1.03 μm, and a tilt angle of 17°. The vibrations in two directions have nearly a 180° phase shift. This anti-phase vibration reduces the ellipse locus to a straight line, which agrees with the simulation results that state that only tangential mode vibrations occur at the 1st natural frequency. The tilt angle of the trajectory is caused by the asymmetry in the design of the tool tip and tool holder.

At the resonant frequency at 28 kHz the vibration modes include both tangential and normal vibrations resulting in comparable vibration amplitudes in two directions as shown in Fig. 11(a). The tangential vibration amplitude is 8.79 μm while the normal

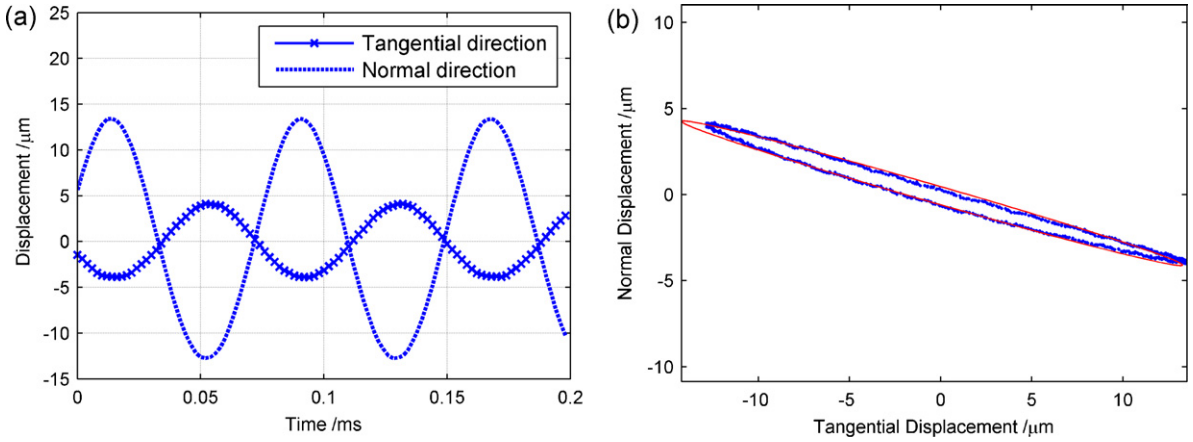

Fig. 10. (a) Recorded displacement at 13 kHz and (b) vibration trajectory at 13 kHz.

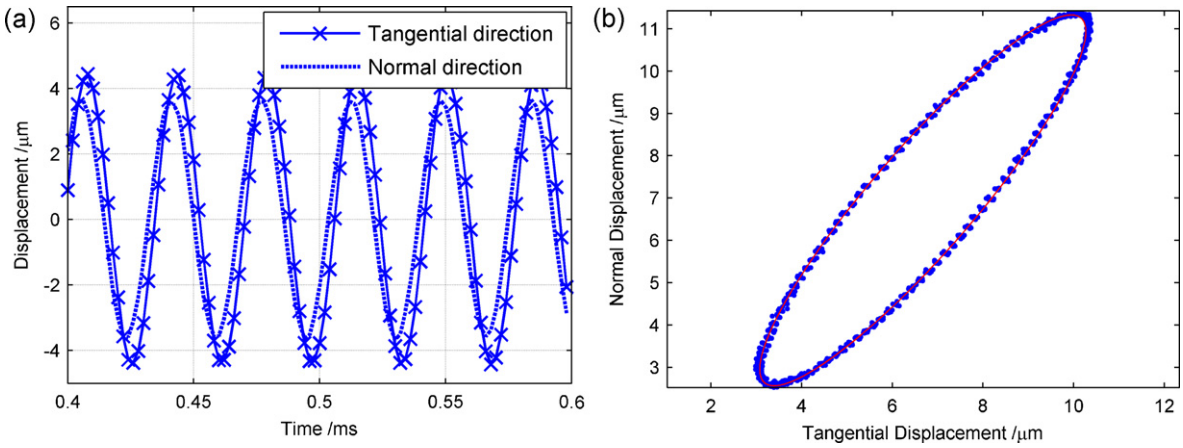

Fig. 11. (a) Recorded displacement at 28 kHz and (b) vibration trajectory at 28 kHz.

vibration amplitude is 7.28 μm. The trajectory is again fitted into an ellipse with a major axis of 11.09 μm, a minor axis of 2.34 μm, and a tilt angle of 39° (Fig. 11(b)).

The resonant vibration at 28 kHz is of particular interest, since it meets the requirements of an elliptical trajectory at an ultrasonic frequency for the elliptical vibration texturing process. The vibration behavior at this natural frequency is further analyzed by changing the phase shift between the two excitation signals but keeping the excitation frequency and amplitudes constant. The results are shown in Fig. 12. The input phase shift affects the vibration amplitudes in both the tangential and normal directions. The tangential vibration amplitude reaches its maximum at a 60° phase angle, which agrees with the V-shape angle of the TMG design. The normal vibration amplitude reaches its maximum at the 0 phase angle, since pure symmetric vibrations in the two transducers produce the largest normal direction motions, which corresponds to the in-phase mode in the previous analysis. Different representative shapes of the elliptical trajectory are plotted in Fig. 13. The tangential vibration amplitude has a maximal value at the phase angle of 60°, while the normal vibration amplitude at 0°. These conclusions agree with the analysis above. If the vibration trajectory is approximated by an ellipse, the ratio between the major axis over the minor axis is determined by the output phase shown in Fig. 12. A larger output phase angle indicates a smaller aspect ratio between the major and minor axes, which turns the locus more toward a circle (where the ratio becomes 1). At a 0° input phase angle, the output phase angle is around 50°. The trajectory has the least aspect ratio and the area included in the ellipse is the largest. At a 150° input phase angle, the input phase angle is near 0°, which turns the ellipse into a straight line.

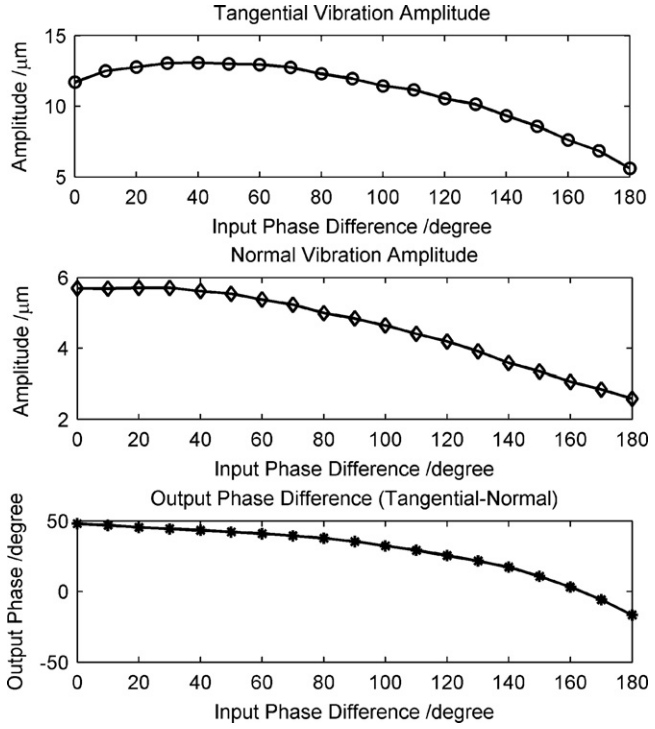

Fig. 12. Input phase influence on the vibration amplitude and phase.

6. Preliminary test results

The newly developed TMG was integrated into a desktop milling/drilling/turning machine as shown in Fig. 14. The *X*–*Y* stage with a resolution of 0.25 μm in both directions carries the TMG mounted on a four component Kistler dynamometer. The *Z* axis supports a high speed air spindle and a linear stage with a 1.27 μm resolution. The machine is configured to operate as a lathe in the vertical direction. The workpiece is loaded in the spindle along the *Z* axis. The spindle provides the primary motion for the turning

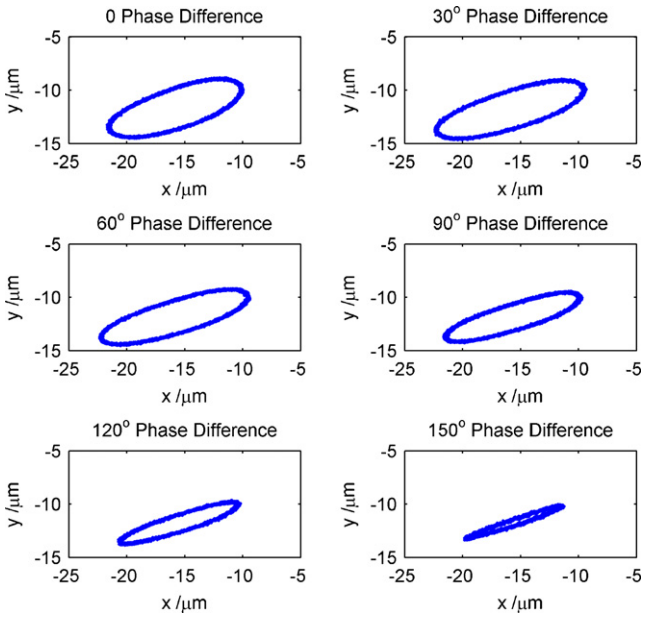

Fig. 13. Ellipse shapes at different phase inputs.

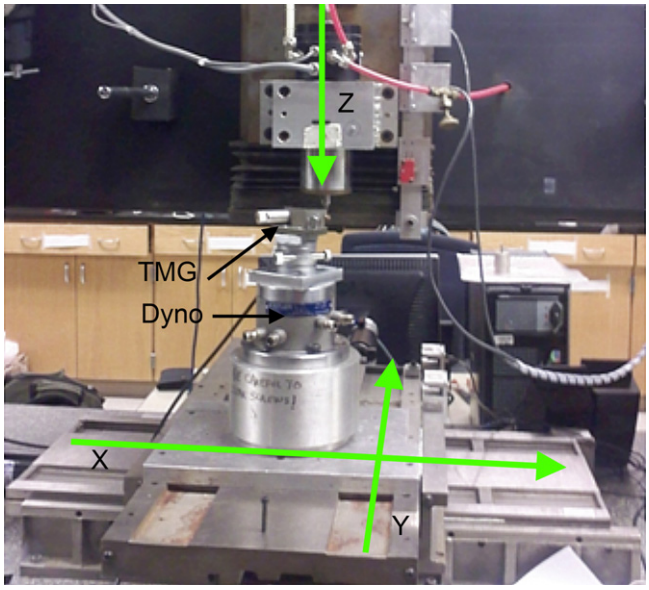

Fig. 14. Turning machine configuration.

operation. The linear motor in the Z axis controls the feed motion while the X–Y stage sets the depth of cut.

A closer look at the experimental setup is shown in Fig. 15. A special rotary fixture is used to change the orientation of the TMG. The workpiece has a diameter of 3 mm (1/8 in.). Commercially available carbide and diamond inserts, whose nose radius is 400 μm and 200 μm respectively, are used. The machine is controlled by a Delta Tau UMAC system, which is capable of controlling up to 32 axes simultaneously with a Turbo PMAC2 CPU running at 80 MHz. A series of cutting tests were performed to verify the concept of the process to fast generate structured surfaces in the turning operation. The machined surfaces were examined using a Zygo white-light interferometer.

One example of the machined surfaces using the elliptical vibration texturing process is shown in Fig. 16. Such surfaces with carefully designed dimple patterns can be applied in friction reduction applications as well as for the creation of surfaces with hydro-phobic/-philic, reflective, antibacterial and other properties.

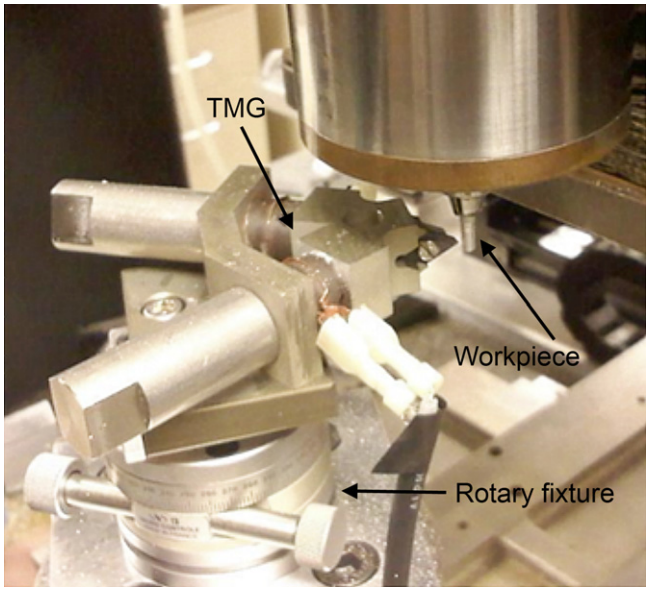

Fig. 15. TMG setup.

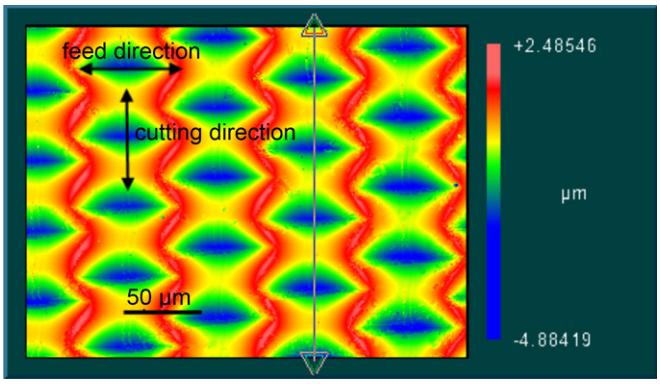

Fig. 16. Surface topography of the textured surface.

In friction applications, for example, the dimple arrays expand the range of the hydrodynamic lubrication regime and substantially reduce the friction coefficient when compared to polished surfaces [18].

The cutting tool used is a commercial diamond insert. The workpiece material is aluminum 6061. The workpiece was first pre-turned without elliptical vibrations, and then textured with the tertiary motion generated by the TMG at 28 kHz at a spindle speed of 7500 rpm, feed rate of 60 μm/rev and a nominal depth-of-cut (DOC) of 2 μm. The experimental conditions are summarized in Table 2.

As shown in Fig. 16, the elliptical vibration texturing process generates arrays of dimple patterns on the machined surface. The dimple shape is a replica of the cutting tool geometry. The distance between dimples in the feed direction is determined by the feed rate, which is 60 μm in this case. The gap in the cutting direction is defined as:

$$l_{cut} = \frac{\pi N R_0}{30 f} \tag{1}$$

where N is the spindle speed; R_0 is workpiece radius; f is the vibration frequency.

A surface profile along a line segment in the cutting direction is obtained, as shown in Fig. 17, which is compared to the theoretical calculation based on the kinematics of the motion. The schematic of the process is shown in Figs. 1 and 2. The height profile shows periodic peaks and valleys due to the elliptical vibration of the cutting tool. The dimples are around 40 μm apart in the cutting direction, which is compared to the calculated value of 42 μm. The average depth of the dimples is 2.5 μm. The differences in the surface profiles between the calculation and experiments, e.g., the dimple depth and width, show that there is a large elastic recovery during the cutting process. Another possible reason for the difference between the simulated and measured results is from the process dynamics. The measured trajectory was recorded without the cutting load. In reality the actual vibration amplitudes changed due to the process damping for different cutting conditions [19]. Further investigations in the modeling of micro cutting mechanics and system dynamics are needed to predict the actual surface topography. A controller could be designed based on these models

Table 2
Experimental conditions.

Process parameter			
Texturing		Pre-turning	
Spindle speed	~7500 rpm	Spindle speed	~12,500 rpm
Feed rate	60 μm/rev	Feed rate	5 μm/rev
Nominal DOC	2 μm	Nominal DOC	10 μm

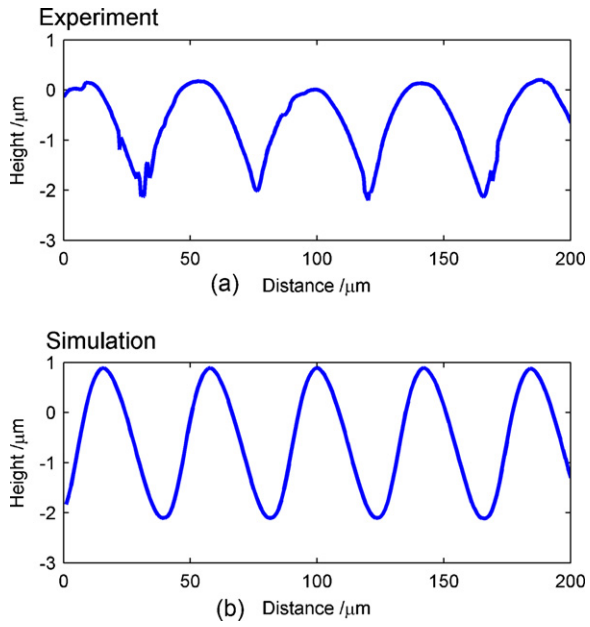

Fig. 17. Surface profile along the cutting direction: (a) experiment and (b) simulation.

to stabilize the vibration amplitudes, for example, by keeping the average cutting force constant.

7. Conclusions

In this paper, an innovative machining method for the fast generation of structured surfaces has been proposed. A design for the tertiary motion generator – TMG, the key component of the process, has been proposed, analyzed and verified. In summary, the following conclusions can be drawn:

- The elliptical vibration texturing process utilizes controlled vibrations of the cutting tool to generate micro/meso-scale features on engineered surfaces. The vibrations are in the cutting and depth-of-cut directions. The process is closely related to the elliptical vibration cutting process.
- The TMG works in the resonant mode, which includes two coupled vibration modes at nearly the same frequency. The device is excited at this coupled resonant frequency to deliver an elliptical trajectory.
- The proposed resonant TMG is integrated into a desktop turning machine to implement the elliptical vibration texturing process in turning operations. Preliminary results, showing micro dimple arrays on an aluminum cylinder, validate the principle and performance of the TMG.

Acknowledgement

This work was supported by the National Science Foundation under Grant number DMI-0600175.

References

[1] Bruzzone AAG, Costa HL, Lonardo PM, Lucca DA. Advances in engineered surfaces for functional performance. CIRP Annals – Manufacturing Technology 2008;57:750–69.
[2] Dornfeld D, Min S, Takeuchi Y. Recent advances in mechanical micromachining. CIRP Annals – Manufacturing Technology 2006;55:745–68.
[3] Hong MS, Ehmann KF. Generation of engineered surfaces by the surface-shaping system. International Journal of Machine Tools and Manufacture 1995;35:1269–90.
[4] Moriwaki T, Shamoto E. Ultraprecision diamond turning of stainless steel by applying ultrasonic vibration. CIRP Annals – Manufacturing Technology 1991;40:559–62.
[5] Shamoto E, Moriwaki T. Study on elliptical vibration cutting. CIRP Annals – Manufacturing Technology 1994;43:35–8.
[6] Moriwaki T, Shamoto E. Ultrasonic elliptical vibration cutting. CIRP Annals – Manufacturing Technology 1995;44:31–4.
[7] Li X, Zhang D. Ultrasonic elliptical vibration transducer driven by single actuator and its application in precision cutting. Journal of Materials Processing Technology 2006;180:91–5.
[8] Shamoto E, Moriwaki T. Ultaprecision diamond cutting of hardened steel by applying elliptical vibration cutting. CIRP Annals – Manufacturing Technology 1999;48:441–4.
[9] Brehl DE, Dow TA. Review of vibration-assisted machining. Precision Engineering 2008;32:153–72.
[10] Cerniway M. Elliptical diamond milling: kinematics, force, and tool wear. MS thesis. North Carolina State University; 2001.
[11] Moriwaki T, Shamoto E, Inoue K. Ultraprecision ductile cutting of glass by applying ultrasonic vibration. CIRP Annals – Manufacturing Technology 1992;41:141–4.
[12] Zhou M, Wang XJ, Ngoi BKA, Gan JGK. Brittle–ductile transition in the diamond cutting of glasses with the aid of ultrasonic vibration. Journal of Materials Processing Technology 2002;121:243–51.
[13] Kim G, Loh B. Machining of micro-channels and pyramid patterns using elliptical vibration cutting. The International Journal of Advanced Manufacturing Technology 2010;49:961–8.
[14] Nath C, Rahman M, Neo KS. A study on ultrasonic elliptical vibration cutting of tungsten carbide. Journal of Materials Processing Technology 2009;209:4459–64.
[15] Kuribayashi Kurosawa M, Kodaira O, Tsuchitoi Y, Higuchi T. Transducer for high speed and large thrust ultrasonic linear motor using two sandwich-type vibrators. IEEE Transactions on Ultrasonics, Ferroelectrics and Frequency Control 1998;45:1188–95.
[16] Zhang F, Chen W, Lin J, Wang Z. Bidirectional linear ultrasonic motor using longitudinal vibrating transducers. IEEE Transactions on Ultrasonics, Ferroelectrics and Frequency Control 2005;52:134–8.
[17] Asumi K, Fukunaga R, Fujimura T, Kurosawa MK. Miniaturization of a V-shape transducer ultrasonic motor. Japanese Journal of Applied Physics 2009:48.
[18] Kovalchenko A, Ajayi O, Erdemir A, Fenske G, Etsion I. The effect of laser texturing of steel surfaces and speed-load parameters on the transition of lubrication regime from boundary to hydrodynamic. Tribology Transactions 2004;47:299–307.
[19] Shamoto E, Suzuki N, Moriwaki T, Naoi Y. Development of ultrasonic elliptical vibration controller for elliptical vibration cutting. CIRP Annals – Manufacturing Technology 2002;51:327–30.